ESAIM: PROCEEDINGS AND SURVEYS, November 2023, Vol. 74, p. 51-62
Editors: Marguerite Zani, Clément Marteau - Journées MAS 2020, Fédération Siméon Poisson (Orléans-Tours),

DYNAMICAL SYSTEMS APPROACHES TO THE STUDY OF CLIMATE WITH APPLICATIONS TO 2022 EXTREME WEATHER EVENTS [*, **]

Davide Faranda [1]

Abstract. Between 1980 and 2020, extreme weather and climate change events have caused, in Europe, up to 520 billion euros in economic losses, according to a 2022 report released by the European Environment Agency. Many weather extreme events such as heatwaves, droughts, tropical cyclones and cold spells will change in frequency and/or intensity due to the ongoing anthropogenic climate change, driving our planet to unprecedented threats. From a theoretical point of view, such extreme events are difficult to characterize because they are rare and they do occur at specific spatiotemporal scales of the dynamics, not necessarily the largest or the smallest of the climate system. Their study requires a framework capable of tracking their probability of occurrence, predictability and persistence. In this manuscript I will describe how dynamical systems theory helps in building numerical and theoretical tools for weather extreme events, using recurrences of patterns termed analogues. These tools can be used to study whether climate change do already affect the dynamics of extremes. Three recent examples will be analysed in details, namely the Argentinian heatwave, the Greek cold spell and the windstorm Malik, all occurred in January 2022.

Résumé. Entre 1980 et 2020, les phénomènes météorologiques extrêmes et le changement climatique ont causé, en Europe, jusqu'à 520 milliards d'euros de pertes économiques, selon un rapport publié en 2022 par l'Agence européenne pour l'environnement. De nombreux événements météorologiques extrêmes tels que les vagues de chaleur, les sécheresses, les cyclones tropicaux et les vagues de froid vont changer de fréquence et/ou d'intensité en raison du changement climatique anthropique en cours, faisant peser sur notre planète des menaces sans précédent. D'un point de vue théorique, ces événements extrêmes sont difficiles à caractériser car ils sont rares et se produisent à des échelles spatio-temporelles spécifiques de la dynamique, pas nécessairement les plus grandes ou les plus petites du système climatique. Leur étude nécessite un cadre capable de suivre leur probabilité d'occurrence, leur prévisibilité et leur persistance. Dans ce manuscrit, je décrirai comment la théorie des systèmes dynamiques aide à construire des outils numériques et théoriques pour les événements météorologiques extrêmes, en utilisant des récurrences de modèles appelés analogues. Ces outils peuvent être utilisés pour étudier si le changement climatique affecte déjà la dynamique des extrêmes. Trois exemples récents seront analysés en détail, à savoir la canicule argentine, la vague de froid grecque et la tempête de vent Malik, toutes survenues en janvier 2022.

---

* *This study is supported by the INSU CNRS LEFE-MANU grant DINCLIC and the ANR-TERC BOREAS.*

** *This study has received funding from the European Union's Horizon 2020 research and innovation programme under grant agreements No 101003469 (XAIDA) and under Marie Skłodowska-Curie grant No. 956396 (EDIPI).*

[1] Laboratoire des Sciences du Climat et de l'Environnement, CEA Saclay l'Orme des Merisiers, UMR 8212 CEA-CNRS-UVSQ, Université Paris-Saclay & IPSL, 91191, Gif-sur-Yvette, France; London Mathematical Laboratory, 8 Margravine Gardens, London, W6 8RH, UK; LMD/IPSL, Ecole Normale Superieure, PSL research University, 75005, Paris, France

Article published online by EDP Sciences and available at https://www.esaim-proc.org or https://doi.org/10.1051/proc/202374051

Introduction

Since the beginning of the 20th century, the need to predict the occurrence and return of geophysical extremes such as heatwaves, storms, floods or droughts has motivated mathematicians to create statistical tools to study these phenomena [20, 21]. Together, these tools constitute the extreme value theory (EVT) [35]. The application of EVT was originally limited to time series. This framework was useful for studying localised physical phenomena such as atmospheric temperature extremes measured at a specific point in space. However, there was no theory to study the chaotic dynamics of spatially extended systems. This is relevant for modelling many geophysical extremes such as the dynamics of cyclones and anticyclones leading to heatwaves, cold-spells and storms, which are extended over areas of few thousands kms and persist several days [46].

In general, geophysical extreme events appear as emergent phenomena in complex systems: their severity is not necessarily linked to the maximization (or minimization) of an observable but rather to their rarity and persistence: they occur in a well defined range of scales which often do not correspond to the smallest (dissipative) or the largest (integral) scale of the atmospheric motions [2, 11, 27]. The precise scales of these phenomena depend on the destabilization of the atmospheric mid-latitude flow due to internal geophysical instabilities, geographical constraints (i.e. the presence of mountain ranges) and external factors (solar activity, seasonality, greenhouse forcing). For geophysical extreme events, traditional statistical extreme value techniques are difficult to apply: while they successfully define a framework to determine the probability of occurrence of events that are large or small with respect to some specific observables (e.g. temperature maxima or minima, precipitations, floods), they are not adapted to deal with persistent or rare phenomena as the extreme regimes of the mid-latitude atmospheric flow [29, 30, 45].

Therefore, while the core of the theory was developed in the 1940s, its extension to dynamical systems, in particular to recurrent events, dates from the early 2000s. Since then, extreme value theory has proven to be a very effective statistical tool for describing, understanding and predicting certain recurrence properties of geophysical variables as well as for estimating the geometric characteristics of boundary sets (attractors). An overview of the emerging application of EVT to dynamical systems is given in [25] This extenstion has required the introduction of a new mathematical formalism based on the definition of extreme events as rare recurrences in phase space of high dimensional systems [12, 16, 17]. The new framework bridges statistics (extreme value theory) and dynamics (dynamical systems theory) by computing instantaneous properties of the geometrical object which hosts the frequency and probability of all physical states reachable by the system, namely the so-called attractor [10].

One of the main theoretical achievements of this methodology is to demonstrate how impacting climate events correspond to rare recurring states in the phase space of the underlying dynamics. These states can be characterized by means of dynamical systems metrics capable of informing about the predictability (local dimension), the persistence and the synchronization (extremal index) of physical states. These metrics have recently provided insights on a number of geophysical phenomena, including transitions between transient metastable states of the mid-latitude circulation [9, 22], palaeoclimate attractors [4, 28], slow earthquake dynamics [19] and changes in mid-latitude atmospheric predictability under global warming [7]. While all these studies target classes of extreme events, the theory of recurrences is also suited to study and analyse properties of a single event. This is of special interest in the field of attribution of weather extremes to climate change.

Extreme event attribution, also known as attribution science, is a relatively new field of study in meteorology and climate science that attempts to measure how ongoing climate change directly affects weather events. A 2004 article in the journal Nature [37] is generally considered the first scientific attribution study. He estimates that human influence at least doubled the risk of a heat wave exceeding the magnitude threshold of the historic 2003 heat wave in Europe. Even though weather extreme events also happened in the past, the science of attribution is geared towards determining whether recent occurrence of extreme events can be enhanced or linked to a warming atmosphere, taking into account also the role of natural variability [40–44]. Attribution studies typically proceed in four steps: (1) measuring the magnitude and frequency of a given event based on observed data, (2) running computer models to compare and verify observational data , (3) run the same models on an Earth baseline without climate change, and (4) use the statistics to analyze the differences between the second and third stages, thereby measuring the direct effect of climate change on the event studied [39]. Heat waves are the easiest weather events to attribute. Climate change may affect the intensity and frequency of extreme weather events differently, for example the 2010 heat wave in Russia was made much more likely but not made more intense [31].

In order to use dynamical systems theory to attribute extreme events to climate change, we target the concurrent atmospheric circulation patterns and search for pattern recurrences in the far (1948-1977) and recent past (1992-2021). Our working hypothesis is that the far past acts as a counterfactual world where the Earth climate was not influenced by anthropogenic forcing when compared to the recent past (the factual world). The choice of a 30 years period for the factual and counterfactual periods ensures having a large statistical sample of *slp* maps to select authentic analogues and to satisfy both the assumptions of stationarity of the climate with respect to anthropogenic climate change while averaging over the interannual and interdecadal natural variability of the atmospheric circulation. Indeed, we have verified that the results do not depend sensibly on the choice of the number of analogues provided that we extract between 25 and 50 analog maps.

We focus on extreme events occurred in 2022 and attribute their circulation drivers to climate change. In particular, we analyze i) the Argentinian heatwave, ii) the Greek cold spell caused by storm Elpis and iii) the windstorm Malik all occurred in 2022 and determine the effects of climate change on these events. The rest of the manuscript is organized as follows. In section 1 we outline the methods and describe the dynamical systems metrics used to perform attribution such as the analogs quality, the predicatibility and the persistence. In section 2 we detail the events analysed and perform the attribution studies. Finally, in section 3 we discuss our results in light of those obtained by the climate scientists community.

1. Methods

Extreme Value Theory (EVT) has been introduced in the study of climate a decade ago [8] and has gained a considerable amount of attention in both the applied mathematics and the climate science communities. It allows to compute recurrence times statistics for climatic systems, but also provides important information on the stability and the predictability of a particular climatic state. This information is contained in indicators that can be estimated via EVT-based methods, namely the instantaneous dimension D and the persistence Θ. The concept of instantaneous dimension is intuitive: for an atmospheric state ζ, e.g. a daily map of sea-level pressure on a given region, the instantaneous dimension $D(\zeta)$ measures the density of similar states. This implies that D can be related to both entropy and trajectory predictability. The stability of the state ζ is measured by $\Theta(\zeta)$ defined as the average persistence time of trajectories around ζ. If the dynamics is stuck in ζ, $\Theta(\zeta) \to \infty$. For quickly changing states ζ, then we have $\Theta = 1$. In general, the more persistent the state, the more the system states will resemble ζ. Details on the computation of D and Θ and on their inference are given in the Appendix A.

We can apply this framework to the study of weather extremes to study anthropogenic-driven climate change of weather patterns [11]. For each of the events, we identify the day where the largest impacts are detected. We then perform a visual inspection of the concurrent weather pattern. In most of the cases, we are interested in a synoptic object, i.e. a cyclone or anticyclone or a couple of these structures. During this identification, we select a region (a longitude/latitude box) that fits the synoptic field that we want to examine. As database we use daily sea level pressure (*slp*) data from the NCEP/NCAR reanalysis [23] over the period 01/01/1948 – 01/02/2022. The data has a horizontal resolution of $2.5° \times 2.5°$. Once fixed the state of interest ζ, which corresponds to a daily map, we scan all the average daily sea-level pressure *slp* maps in two periods: 1948-1977 (counterfactual world) and 1992-2021 (factual world). For both periods we select the best 33 recurrences – also termed analogues in the atmospheric jargon [47] – (quantile 0.997) as the daily *slp* maps minimizing the pointwise euclidean distance with respect to the target ζ. Note that, instead of the euclidean distance, one could use the absolute values of spatial map correlations, but this is not strictly considered a distance metric from the dynamical systems theory viewpoint. To avoid having biased estimation for the factual period, we remove a week around the state ζ from the dates for analogs search. Once obtained the two sets of analogues for the factual and counterfactual periods, we average them out to search for significant differences Δslp. To determine significant changes, we adopt a bootstrap procedure which consists in making a unique pool of dates from both the periods and randomly extracting 1000 times 33 dates, creating the corresponding difference maps and marking as significant only grid point changes above two standard deviations of the bootstrap sample. Conditioning to the dates determined for *slp* fields, we also study the associated 2 meters temperatures $t2m$ and total precipitation maps tp. The bootstrap procedure is repeated on these ensembles to identify significant changes.

Using the framework of dynamical systems described above, we then introduce few metrics to determine the recurrence properties of the field in the counterfactual and factual world. This implies that the metrics introduced below are computed twice with respect to the analogues obtained in the two periods.

- Analogs Quality Q: we can study the typicality of ζ by comparing the euclidean distance of ζ from its analogues with the distances of the analogues from their own analogues. If the value of Q belongs to the same distribution of the values of Q analogues, then typicality is ensured and attribution of ζ can be performed. We establish this by a visual inspection of the violin plots presented in this paper. If instead the Q for the chosen day is larger than that of the analog days, then this is an unprecedented *slp* state and the results for attribution must be taken more carefully. A difference in Q between the counterfactual and factual periods indicate a change in typicality of the event due to climate change.
- Predictability Index D: we can compute the above defined dimension D of the event ζ in both the periods to detect a climate-change induced shift in predictability. Indeed, D is a proxy for the number of degrees of freedom of the field, meaning that the higher the dimension the more unpredictable the next *slp* maps will be. If the dimension D of the chosen day is higher or lower than that of the analogues, then the day will be less or more predictable than its closest dynamical situations.
- Persistence Index Θ: another information derived from the dynamical systems theory is the persistence of a given state. The persistence counts for how many days we are likely to observe a map that is an analogue of the one considered. Once again we will compute Θ for the two different periods and using the analogs as well to detect shifts from the factual to the counterfactual worlds.
- Seasonality of Analogs: we can also simply count the number of analogs in each month to detect whether a given circulation shifts towards earlier or later months. This can have strong thermodynamic implications.

For more information, please refer to [13].

2. Applications

In this section we show, through three examples how to perform the framework of recurrences introduced in dynamical systems theory can be used to attribute extreme events to climate change.

2.1. Argentinian heat wave

A vast stable anticyclone has caused an intense heat wave to South America in January 2022, affecting several countries such as Argentina, Paraguay, Uruguay and southern Bolivia. In particular, Argentina was the country most affected by this event. In Buenos Aires, on 11 January, the maximum temperature of +41.1°C has been recorded, establishing one of the hottest days ever for the capital. On the same day, the thermometer in several provinces of the country such as: Santa Fe, Cordoba, Santiago del Estero, Mendoza, La Rioja and San Juan all recorded highs of over 42°C, reaching as high as 45°C in the city of San Juan. The heatwave managed to push even further south, reaching northern Patagonia in San Antonio Oeste, in the southern province of Buenos Aires, where +42.8°C was recorded, although it failed to beat the previous record of +44.6°C set in January 1980. According to the National Meteorological Service, an exceptional wave like this one has not occurred in about 25 years [36]. The event has caused a number of problems in large urban centres, where the excessive use of air conditioning systems has led to the blackout of the most densely populated cities, leaving hundreds of thousands of people without electricity. The authorities issued several red and orange heat-stroke alerts for the country's central and northern provinces, indicating a high health risk for the population.

We now show how the recurrence method can be used to give hints on the role of climate change in triggering the temperature records. Figure 1 shows the analogs attribution results for January 10, 2022. This date has been chosen as the one when most of the temperature records were broken. First, we note that the *slp* field (a) of the event exhibits two large anticyclonic structures over the Pacific and the Atlantic oceans and a relatively low pressure over Argentina. This causes advection of air masses from the West. This air mass is of marine origin and originates from the Pacific Ocean. It is then lifted above the Andes mountain range. On the Chilean side of the Andes, the lift produces a Stau effect and precipitation. The air mass is dryer when it descends on the Argentinian side of the Andes (Foehn effect) and this causes an additional warming. The analogs found for the counterfactual (b) vs factual (c) periods exhibit a very similar structure to the target field. The difference between the average *slp* maps displayed in (c) and (b) is shown in panel (d). There is a significant (color filled areas) increase of the *slp* dipole in the recent period, favoring the advection of warm air from the West. We observe that the associated temperatures (e-g) are significantly warmer (h) in the recent period (>5°C), especially over land and Argentina. Higher temperatures could be due to the increase in the heat low with climate change, which is a thermal process and not a dynamical one. But the heat low location could also be fostered by drought increase and feedbacks, and have dynamical effects. Precipitations associated with this state (i-l) are lower in the recent period over the southern part of Argentina and Chili, while there is a tendency of increasing precipitation in Brasil with these dynamical states. The analogs quality (m) shows that this circulation pattern becomes more common in the recent than in the past period, because the quality Q of the event (blue dot) is more in the bulk of the distribution of the analogs in the factual than in the counterfactual period. The fact that the quality of the event reflects the median quality of its analogs ensures that the possibility to attribute this event. Note also that the distribution of the analogs quality in the factual world has two modes, meaning that the analogues belong to two different groups, with slightly different circulation patterns. This is possibly due to the large extent of the geographical region used for this case. We do not detect large significant changes in the predictability D (n) and persistence Θ (o) of the state, although there is a modest increase in the persistence of the recent analogues. Finally, we observe a large seasonality shifts of the analogs in the warmer season (the Boreal winter) in the present period with respect to the past period. This shift can greatly enhance the heat associated with this atmospheric circulations as they tend to appear now in the warmer months.

2.2. **Greek cold spell - Storm Elpis**

The winter storm called Elpis by the Greek Meteorological Service [18], has frozen several cities in the country, with temperatures below 0ºC and heavy snowfalls. In the capital, Athens, the increasingly thick snow has quickly settled on the marble columns of the ancient Acropolis covering the hill where the Parthenon stands. The storm Elpis caused a historical snowstorm in Athens on 24/25-01-2022, as locally the snow reached 60-80cm or more in mountainous areas of Greece. The weather event was even more impressive because the snow has fallen at sea level, in places such as Santorini, Mykonos, Syros, Naxos, Tinos and Andros. The frost led to the closure of parliament and schools. Air and sea transport was not impacted, but road and railways connection in the capital and cross-country were disrupted. According to Costas Lagouvardos [32], research director of the National Observatory of Athens, the last time the Greek capital had faced such severe weather conditions was in 1968. The cold wave - which has also spread to the islands in the Aegean Sea, covered by a blanket of snow, and as far away as Crete - causing huge disruptions to the population in various parts of the country, with electrical blackouts and road traffic problems. Storm Elpis also affected Turkey and Israel with heavy historical snowfalls in both the city of Istanbul and Jerusalem.

The attribution analysis for the Greek cold spell is shown, for the 24th of January, in Figure 2. The *slp* field (a) of the event shows a dipole structure with an high pressure system over the Northern Balkan peninsula and a low pressure system over the Black sea with a secondary minimum over Crete. This structure favors the advection of cold air masses from Eastern Europe into the Mediterranean. This air mass is of continental origin (Siberia) and it produces the cyclogenesis over the Greek islands and local convective precipitations, i.e. the snow-see effect, described in [5,6]. The analogs found for the counterfactual (b) vs factual (c) periods exhibit a rather different structure than the target field as they do not show a deep *slp* minimum over the Black sea. The difference between the average *slp* maps displayed in (c) and (b) is shown in panel (d). There is a significant (color filled areas) increase of the *slp* cyclonic structure over Greece in the recent period, favoring precipitation in the area. We observe that the associated temperatures (e-g) are significantly lower (h) in the recent period (<-3°C) over the Balkans and significantly higher over the Mediterranean basin. Precipitations associated with this state (i-l) are significantly more abundant in the factual world in a narrow band which includes Istanbul. The analogs quality shows that this circulation pattern becomes more common in the recent than in the past period, as the quality Q of the event (blue dot) is more in the bulk of the distribution of the analogs in the factual than in the counterfactual period. However, the analogs quality of the event is in general out of the distribution of the analogs. This could be due to the fact that analogs do not reproduce the *slp* minimum over the Black sea, a determinant factor to advect cold air to the Aegean sea. We do detect a significant shift towards increasing the predictability D in the factual period (n) and decreasing the persistence Θ (o). Finally, we observe a large seasonality shift (p) of the analogs in winter, especially in the month of February. This greatly enhances the cold advection associated with these states as they tend to appear in the months when Siberia and the Balkans are cooler.

2.3. Storm Malik

Storm Malik has swept across much of Northern Europe, causing extensive damage, casualties and injuries from the 27 to the 29 January 2022. Numerous damages were left behind by the hurricane-force winds in England and Scotland, where wind gusts reached (and even sometimes exceeded) 130 km/h. Several tens of thousands of homes have been left without electricity. Important road-traffic disruptions were caused by the numerous fallen trees along the roads. The fall of a tree felled by the strong wind in Aberdeen, Scotland, caused the death of a 60-year-old woman, trapped under the tree. At least one person also died in Denmark: a 78-year-old woman was hit by a door while standing in the street. As in the other Scandinavian countries, there was considerable damage to traffic and numerous power cuts [3].

We show the attribution analysis for Storm Malik in Figure 3. The *slp* pattern for Malik on 28-01-2022 consists of a large cyclonic structure center over Iceland and an anticyclone over the English Channel. This causes strong wind in all the areas where the pressure gradient is maximum, so in Scotland and Norway. The analogs field for the counterfactual (b) and factual (c) periods shows a dipolar structure but the position of the *slp* minimum is located on the Western side of Iceland rather than on the North-Eastern side of the island. The Δslp map (d) shows large areas of significant differences with an intensification of both the cyclonic and anticyclonic structures, leading to stronger winds especially over Scotland and Iceland. We observe that the associated temperatures (e-g) are significantly higher over Greenland and the Arctic ocean as well as over England and France during the recent times. The recent events tend to be associated with Arctic winter temperature anomalies. Precipitations associated with this state (i-l) are significantly more abundant in the factual world on the island of Iceland but no significant shifts are detected over the United Kingdom. The analogs quality tends to improve in the recent period (m) whereas the event looks at the edge of the analogs distribution for the counterfactual period. There is a comparable shift in the predictability D (n), while the persistence increase in the factual world (o). This can enhance the impacts on infrastructure as intense winds and wind gusts insist on the same are for longer. From (n) we can derive an increase of persistence of about two hours on average in the factual world. Finally we observe (p) an important shift of these storms towards the early months of Winter and Spring, while in the counterfactual worlds they tend to happen mostly in Autumn.

3. Discussion and Perspectives

In this study we have shown how dynamical systems theory and in particularly recurrences can be leveraged to the study of weather extreme events such as cold spells, heat waves and windstorms. The main idea is to split the dataset – here the NCEP reanalyses – into two contiguous segments acting as counterfactual and factual worlds. The counterfactual world has been here selected as the period 1948-1977 as the one less influenced by the climate change, while the factual world is the recent past 1992-2021. With this approach we have investigated whether three recent extreme events such as the Argentinian heatwave, the Greek cold-spell associated with the storm Elpis and the storm Malik have been influenced by climate change.

For the Argentinian Heatwave, the circulation pattern associated with the heat peak in Argentina presents a bipolar anticyclonic-cyclonic structure which favors advection of warm dry air from the west to the country. This dipole deepens in the factual period w.r.t the counterfactual periods favoring a larger warm advection. Finally the analogs shift in the warmer months of December, January, February in the recent period, producing extreme warming. This is consistent with the IPCC AR6 [1] report which states that heatwaves will be more likely in a changing climate.

For the Greek cold spell driven by the storm Elpis, we have discussed the exceptional and unprecedented nature of this event which has been driven by a deep low pressure minimum over the Black sea, favoring the advection of cold air in the Aegean sea with a secondary cyclogenisis. While cold spells are decreasing in present climate due to the action of the global warming, the increased likelihood of this circulation patterns in the coldest months could still trigger intense cold spells and snowfalls in the area in the present and future climates. Similar results and conclusion can be found also in [5, 6].

Finally, the results obtained for Storm Malik show an increasing pressure dipole leading to more intense winds, in line with what stated by the IPCC, namely that future climate will be more dominated by more cyclonic circulation patterns and increase in cyclonicity and stronger westerlies.

This work comes with some caveats: i) the quality of reanalyses data before the satellite era (roughly 1979) is poor and this may especially affect the representation of cyclones and anticyclones; ii) the NCEP reanalyses have a coarse resolution and they can have large biases in the representation of fields showing small scale features such as $t2m$ and tp. Despite these caveats, our results look statistically robust and they allow to introduce also the concept that attribution results must be taken with an extremely careful approach because the event can be unprecedented and therefore having no correspondence in the factual and counterfactual worlds. They also suggest the prominent role of the atmospheric circulation in triggering and enhancing the characteristics of extreme events as already highlighted in [33, 34, 48].

A. Local dimension D and persistence Θ

Local dimension D is computed by applying extreme value statistics to Poincaré recurrences of a state ζ [24]. ζ, here represented by a sea-level pressure longitude-latitude map, is a reference point in an appropriately defined phase space. Here, the trajectories in this phase space are successions of daily sea-level pressure maps in a similar fashion as described in [10]. We then compute the probability that the trajectory returns close to ζ, namely within a ball of radius ϵ centered on ζ. This probability, which gives the distribution of the recurrences (analogues) of ζ, has been studied first in [14] and obeys an extreme value distribution. In order to compute this probability, we first calculate the distances between ζ and all other points within our dataset as:

$$g(x(t)) = -\log(\text{dist}(x(t), \zeta)) \tag{1}$$

where $\text{dist}(x(t), \zeta)$ is the Euclidean distance of SLP maps between each timestep $x(t)$ and ζ. The Freitas-Freitas-Todd theorem [15], modified by Lucarini et al. [26], states that the probability of recurrences, namely of $x(t)$ to fall inside a ball of radius ϵ and centered at ζ, converges to a Generalized Pareto Distribution:

$$P(z > s(q)) \simeq \exp\left[-\vartheta(\zeta)\frac{z - \mu(\zeta)}{\sigma(\zeta)}\right] \tag{2}$$

where $z = g(x(t))$. The radius ϵ is related to a threshold *s(q)* of the time series of the distances computed as Eq. (1) by $\epsilon = \exp(-s(q))$. Due to the application of the -log, the exceedances of the threshold are the points that fall within the radius ϵ from ζ. In this work we take q as a high quantile of our distance timeseries. The local dimension D is simply obtained as: $\sigma = 1/D\zeta)$.

We fit a Generalized Pareto Distribution to the exceedances using the Maximum Likelihood estimator. We also have tested two other methods, the Method of Moments and L-moments, and we have found similar results, namely that when the differences between D in factual and counterfactual periods are statistically significant for a method, they also are so for the others.

The extremal index ϑ is an adimensional parameter between 0 and 1. Its inverse $\Theta = 1/\vartheta$ can be interpreted as the mean residence time of phase-space trajectories within a radius ϵ around ζ in units of the timestep of the data being used, namely a measure of persistence θ. We compute ϑ using the Suveges [38] estimator.

References

[1] R. P. Allan, E. Hawkins, N. Bellouin, and B. Collins. Ipcc, 2021: Summary for policymakers. 2021.

[2] M. C. Alvarez-Castro, D. Faranda, and P. Yiou. Atmospheric dynamics leading to west european summer hot temperatures since 1851. *Complexity*, 2018, 2018.

[3] BBC.

[4] M. Brunetti, J. Kasparian, and C. Vérard. Co-existing climate attractors in a coupled aquaplanet. *Climate Dynamics*, 53(9):6293–6308, 2019.

[5] M. D'errico, P. Yiou, C. Nardini, F. Lunkeit, and D. Faranda. Warmer Mediterranean temperatures do not decrease snowy cold spell intensity over Italy. 2019.

[6] D. Faranda. An attempt to explain recent changes in european snowfall extremes. *Weather and Climate Dynamics*, 1(2):445–458, 2020.

[7] D. Faranda, M. C. Alvarez-Castro, G. Messori, D. Rodrigues, and P. Yiou. The hammam effect or how a warm ocean enhances large scale atmospheric predictability. *Nature communications*, 10(1):1316, 2019.

[8] D. Faranda, J. M. Freitas, V. Lucarini, G. Turchetti, and S. Vaienti. Extreme value statistics for dynamical systems with noise. *Nonlinearity*, 26(9):2597, 2013.

[9] D. Faranda, G. Messori, M. C. Alvarez-Castro, and P. Yiou. Dynamical properties and extremes of northern hemisphere climate fields over the past 60 years. *Nonlinear Processes in Geophysics*, 24(4):713, 2017.

[10] D. Faranda, G. Messori, and P. Yiou. Dynamical proxies of North Atlantic predictability and extremes. *Scientific reports*, 7:41278, 2017.

[11] D. Faranda, G. Messori, and P. Yiou. Diagnosing concurrent drivers of weather extremes: application to warm and cold days in North America. *Climate Dynamics*, 54(3):2187–2201, 2020. ISBN: 1432-0894 Publisher: Springer.

[12] D. Faranda and S. Vaienti. Correlation dimension and phase space contraction via extreme value theory. *Chaos: An Interdisciplinary Journal of Nonlinear Science*, 28(4):041103, 2018.

[13] D. Faranda, M. Vrac, P. Yiou, A. Jézéquel, and S. Thao. Changes in future synoptic circulation patterns: consequences for extreme event attribution. *Geophys. Res. Lett.*, 47(15):e2020GL088002, 2020. ISBN: 0094-8276 Publisher: Wiley Online Library.

[14] A. C. M. Freitas and J. M. Freitas. On the link between dependence and independence in extreme value theory for dynamical systems. *Statistics & Probability Letters*, 78(9):1088–1093, 2008.

[15] A. C. M. Freitas, J. M. Freitas, and M. Todd. Hitting time statistics and extreme value theory. *Probability Theory and Related Fields*, 147(3):675–710, 2010.

[16] A. C. M. Freitas, J. M. Freitas, and M. Todd. The extremal index, hitting time statistics and periodicity. *Advances in Mathematics*, 231(5):2626–2665, 2012.

[17] A. C. M. Freitas, J. M. Freitas, and S. Vaienti. Extreme Value Laws for sequences of intermittent maps. *arXiv preprint arXiv:1605.06287*, 2016.

[18] GreekReporter. Athens snowstorm worst in fourteen years. https://greekreporter.com/2022/01/27/snowstorm-greece-worst-14-years/, 2022. Accessed: 2022-02-15.

[19] A. Gualandi, J.-P. Avouac, S. Michel, and D. Faranda. The predictable chaos of slow earthquakes. *Science advances*, 6(27):eaaz5548, 2020.

[20] E. J. Gumbel. Les valeurs extrêmes des distributions statistiques. In *Annales de l'institut Henri Poincaré*, volume 5, pages 115–158, 1935.

[21] H. L. Harter. A bibliography of extreme-value theory. *International Statistical Review/Revue Internationale de Statistique*, pages 279–306, 1978.

[22] A. Hochman, S. Scher, J. Quinting, J. G. Pinto, and G. Messori. A New View of Heat Wave Dynamics and Predictability over the Eastern Mediterranean. *Earth Syst. Dynam. Discuss.*, 2020:1–29, 2020. Publisher: Copernicus Publications.

[23] E. Kalnay, M. Kanamitsu, R. Kistler, W. Collins, D. Deaven, L. Gandin, M. Iredell, S. Saha, G. White, J. Woollen, Y. Zhu, M. Chelliah, W. Ebisuzaki, W. Higgins, J. Janowiak, K. C. Mo, C. Ropelewski, J. Wang, A. Leetmaa, R. Reynolds, R. Jenne, and D. Joseph. The NCEP/NCAR 40-Year Reanalysis Project. *Bulletin of the American Meteorological Society*, 77(3):437–472, Mar. 1996.

[24] V. Lucarini, D. Faranda, J. M. M. de Freitas, M. Holland, T. Kuna, M. Nicol, M. Todd, S. Vaienti, et al. *Extremes and recurrence in dynamical systems*. John Wiley & Sons, 2016.

[25] V. Lucarini, D. Faranda, A. C. M. Freitas, J. M. Freitas, M. Holland, T. Kuna, M. Nicol, M. Todd, and S. Vaienti. *Extremes and recurrence in dynamical systems*. John Wiley & Sons, 2016.

[26] V. Lucarini, D. Faranda, and J. Wouters. Universal behaviour of extreme value statistics for selected observables of dynamical systems. *Journal of statistical physics*, 147(1):63–73, 2012.

[27] G. Messori, R. Caballero, and D. Faranda. A dynamical systems approach to studying midlatitude weather extremes. *Geophysical Research Letters*, 44(7):3346–3354, 2017.

[28] G. Messori and D. Faranda. Characterising and comparing different palaeoclimates with dynamical systems theory. *Climate of the Past*, 17(1):545–563, 2021.

[29] P. Naveau, R. Huser, P. Ribereau, and A. Hannart. Modeling jointly low, moderate, and heavy rainfall intensities without a threshold selection. *Water Resources Research*, 52(4):2753–2769, 2016.

[30] P. Naveau, A. Ribes, F. Zwiers, A. Hannart, A. Tuel, and P. Yiou. Revising return periods for record events in a climate event attribution context. *Journal of Climate*, 31(9):3411–3422, 2018.

[31] F. E. Otto, N. Massey, G. J. Van Oldenborgh, R. G. Jones, and M. R. Allen. Reconciling two approaches to attribution of the 2010 Russian heat wave. *Geophysical Research Letters*, 39(4), 2012.

[32] RTE. Worst snow storm in over a decade halts covid vaccinations in athens. https://www.rte.ie/news/world/2021/0216/1197514-greece-us-weather/, 2022. Accessed: 2022-02-15.

[33] T. G. Shepherd. Storyline approach to the construction of regional climate change information. *Proceedings of the Royal Society A*, 475(2225):20190013, 2019.

[34] T. G. Shepherd, E. Boyd, R. A. Calel, S. C. Chapman, S. Dessai, I. M. Dima-West, H. J. Fowler, R. James, D. Maraun, O. Martius, C. A. Senior, A. H. Sobel, D. A. Stainforth, S. F. B. Tett, K. E. Trenberth, B. J. J. M. van den Hurk, N. W. Watkins, R. L. Wilby, and D. A. Zenghelis. Storylines: an alternative approach to representing uncertainty in physical aspects of climate change. *Climatic Change*, 151(3):555–571, Dec. 2018.

[35] R. L. Smith. Extreme value theory. *Handbook of applicable mathematics*, 7:437–471, 1990.

[36] SMN. Más de 75 récords de temperatura en un enero de calor extremo. https://www.smn.gob.ar/noticias/mas-de-75-records-de-temperatura-en-un-enero-de-calor-extremo, 2022. Accessed: 2022-02-14.

[37] P. A. Stott, D. A. Stone, and M. R. Allen. Human contribution to the european heatwave of 2003. *Nature*, 432(7017):610–614, 2004.

[38] M. Süveges. Likelihood estimation of the extremal index. *Extremes*, 10(1-2):41–55, 2007. ISBN: 1386-1999 Publisher: Springer.

[39] K. E. Trenberth, J. T. Fasullo, and T. G. Shepherd. Attribution of climate extreme events. *Nature Clim. Change*, 5(8):725–730, Aug. 2015.

[40] G. J. Van Oldenborgh, A. Van Urk, and M. Allen. The absence of a role of climate change in the 2011 Thailand floods. *Bull. Amer. Meteor. Soc*, 93:1047–1049, 2012.

[41] G. J. Van Oldenborgh, A. van Urk, and M. Allen. The absence of a role of climate change in the 2011 Thailand floods [in "Explaining Extreme Events of 2011 from a Climate Perspective"]. *Bulletin of the American Meteorological Society*, 93(7):1047–1049, 2012.

[42] R. Vautard, A. Colette, E. Van Meijgaard, F. Meleux, G. Jan van Oldenborgh, F. Otto, I. Tobin, and P. Yiou. Attribution of Wintertime Anticyclonic Stagnation Contributing to Air Pollution in Western Europe. *Bulletin of the American Meteorological Society*, 99(1):S70–S75, 2018.

[43] R. Vautard and P. Yiou. ATTRIBUTION Robustness of warming attribution. *Nature Climate Change*, 2(1):26–27, 2012.

[44] R. Vautard, P. Yiou, F. Otto, P. Stott, N. Christidis, G. J. v. Oldenborgh, and N. Schaller. Attribution of human-induced dynamical and thermodynamical contributions in extreme weather events. *Environmental Research Letters*, 11(11):114009, 2016.

[45] M. Vrac. Multivariate bias adjustment of high-dimensional climate simulations: the Rank Resampling for Distributions and Dependences (R 2 D 2) bias correction. *Hydrology and Earth System Sciences*, 22(6):3175, 2018.

[46] J. M. Wallace, C. Smith, and Q. R. Jiang. Spatial Patterns of Atmosphere Ocean Interaction in the Northern Winter. *JOURNAL OF CLIMATE*, 3(9):990–998, 1990.

[47] P. Yiou, T. Salameh, P. Drobinski, L. Menut, R. Vautard, and M. Vrac. Ensemble reconstruction of the atmospheric column from surface pressure using analogues. *Clim. Dyn.*, 41(5-6):1333–1344, 2013.

[48] G. Zappa and T. G. Shepherd. Storylines of atmospheric circulation change for European regional climate impact assessment. *Journal of Climate*, 30(16):6561–6577, 2017.

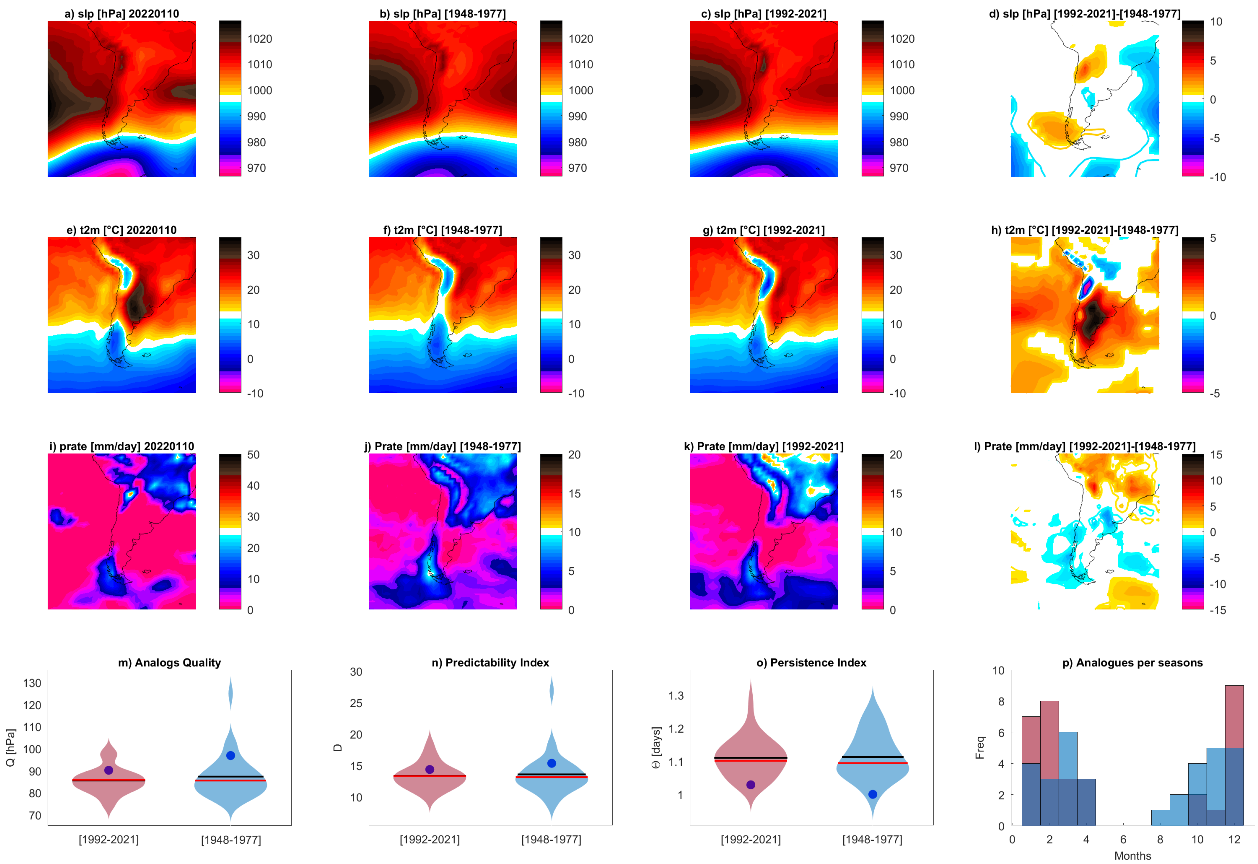

FIGURE 1. Attribution for the Argentinian Heatwave on the day of the heat peak, namely 10-01-2022. Daily mean sea-level pressure slp (a), 2-meter temperatures $t2m$ (e) and total precipitation tp (i) on the day of the event. Average of the 33 sea-level pressure analogs found for the counterfactual [1948-1977] (b) and factual [1992-2021] (c) periods and corresponding 2-meter temperatures (f,g) and daily precipitation rate (j,k). Δslp (d), $\Delta t2m$ (h) and Δtp (i) between factual and counterfactual periods: colored-filled areas show significant anomalies with respect to the bootstrap procedure. Violin plots for counterfactual (blue) and factual (pink) periods for the Analogs Quality Q (m) the Predictability index D (n), the Persistence index Θ (o) and the distribution of analogs in each month (p). Values for the selected day are marked by a blue dot.

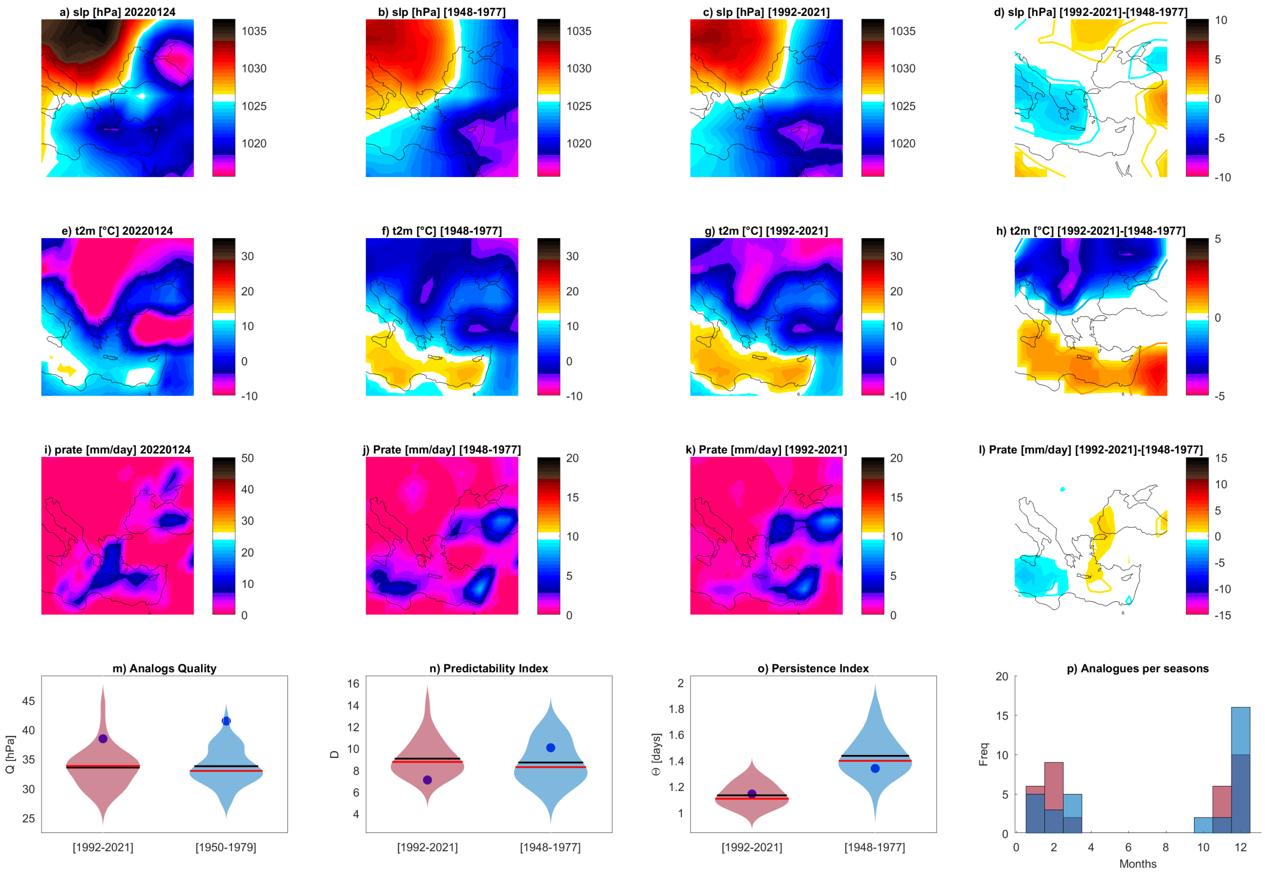

Figure 2. Attribution for the Greek cold spell on the day of the heaviest snowfalls, namely 24-01-2022. Daily mean sea-level pressure slp (a), 2-meter temperatures $t2m$ (e) and total precipitation tp (i) on the day of the event. Average of the 33 sea-level pressure analogs found for the counterfactual [1948-1977] (b) and factual [1992-2021] (c) periods and corresponding 2-meter temperatures (f,g) and daily precipitation rate (j,k). Δslp (d), $\Delta t2m$ (h) and Δtp (i) between factual and counterfactual periods: colored-filled areas show significant anomalies with respect to the bootstrap procedure. Violin plots for counterfactual (blue) and factual (pink) periods for the Analogs Quality Q (m) the Predictability index D (n), the Persistence index Θ (o) and the distribution of analogs in each month (p). Values for the selected day are marked by a blue dot.

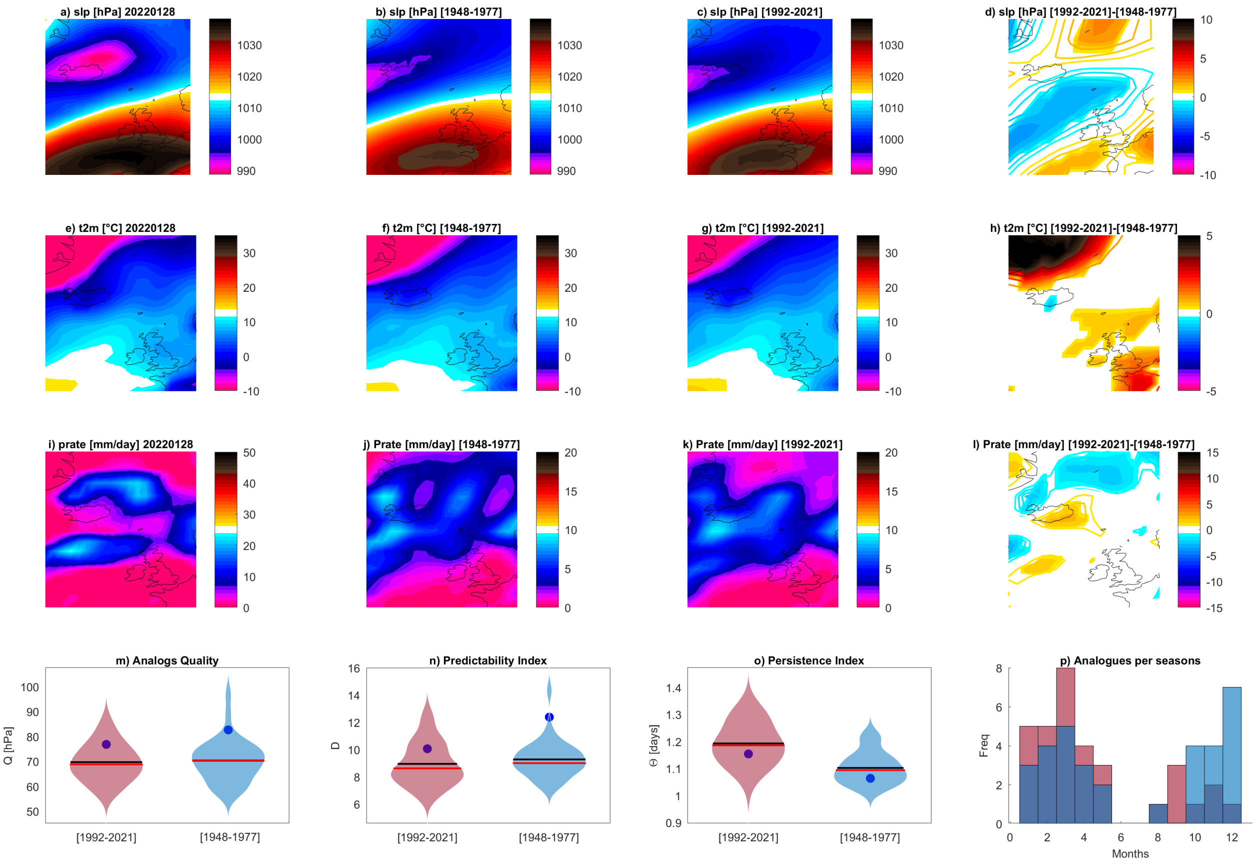

FIGURE 3. Attribution for the Storm Malik on 28-01-2022. Daily mean sea-level pressure *slp* (a), 2-meter temperatures *t2m* (e) and total precipitation *tp* (i) on the day of the event. Average of the 33 sea-level pressure analogs found for the counterfactual [1948-1977] (b) and factual [1992-2021] (c) periods and corresponding 2-meter temperatures (f,g) and daily precipitation rate (j,k). Δslp (d), $\Delta t2m$ (h) and Δtp (i) between factual and counterfactual periods: colored-filled areas show significant anomalies with respect to the bootstrap procedure. Violin plots for counterfactual (blue) and factual (pink) periods for the Analogs Quality Q (m) the Predictability index D (n), the Persistence index Θ (o) and the distribution of analogs in each month (p). Values for the selected day are marked by a blue dot.